Proceedings of the 2006 IASME/WSEAS International Conference on Continuum Mechanics, Chalkida, Greece, May 11-13, 2006 (pp73-78)

On the rheological modeling of blood flow around a clot

TOMÁŠ BODNÁR
Czech Technical University in Prague
Faculty of Mechanical Engineering
Department of Technical Mathematics
Karlovo Náměstí 13, 121 35 Prague 2
CZECH REPUBLIC

ADÉLIA SEQUEIRA
Instituto Superior Técnico
Department of Mathematics
Center for Mathematics and its Applications
Av. Rovisco Pais, 1049–001 Lisbon
PORTUGAL

Abstract: The aim of this paper is to present a possible approach to modeling the influence of clot formation on blood flow in a vessel. The modeling framework adopted in this work is based on a modification of the fluid viscosity within the clot area. A non-Newtonian blood flow model in a three-dimensional straight vessel is considered and its numerical solution is obtained using a finite-volume method. Finally, a qualitative analysis of the results is presented together with some guidelines for future coupling with a biochemical model.

Key–Words: Non-Newtonian fluid, blood flow, coagulation, clot, finite-volume method.

1 Introduction

Blood coagulation is one of the basic defense mechanisms preventing the loss of blood following a vascular injury. When the endothelium is damaged, blood platelets get activated and a complex sequence of chemical reactions occurs at the site of trauma. Activation of the coagulation cascade is triggered by the release of tissue factor from the site of injury and results in the generation of thrombin. Thrombin converts soluble fibrinogen into the insoluble fibrin that forms the matrix of a blood clot.

This is a very rough description of the biochemical processes leading to clot formation. A more detailed description is beyond the scope of this paper and the reader is referred to the literature on the subject. The essential information to understand the approach adopted in this work can be found in the review paper [1] which includes an extensive bibliography on the subject. Thus, only a few references will be given here. The basic phenomenology of blood coagulation is described e.g. in [4], [10] or [6]. Many mathematical models of blood coagulation processes have been developed so far. In the context of this work the most important references are [14], [15] which include a simple 8-equation model for the intrinsic coagulation pathway simulation. Some more complex models including extrinsic tissue-factor coagulation pathway have been developed in [7], [5], [13], [8].

Once the clot is formed, it acts as a mechanical obstacle in blood flow. The clot is built from the blood constituents, however it has significantly different material properties. The mechanical model of clot used here is based on the assumption that both blood and clot are incompressible viscous (or possibly viscoelastic) fluids. In this case the same mathematical description can be used for both fluids, while a model parameter set is used for blood and a distinct one for clot. We assume that the clot has significantly higher viscosity than blood. This approach was proposed in [2] using a shear-thinning viscoelastic model and also in combination with biochemistry in [1].

2 Governing Equations

Blood is a complex fluid which in large and medium vessels can be modeled as a Newtonian liquid. However, in smaller vessels, with diameters comparable with those of the cells, blood behaves as a shear-thinning and viscoelastic fluid (see section 2.4 for more details). In this work we consider the simple case where blood is modeled as a generalized Newtonian fluid with shear-thinning viscosity.

2.1 Basic balance laws

Mass and momentum balance laws for an incompressible viscous fluid can be written in the following general form:

$$\operatorname{div} \boldsymbol{u} = 0 \tag{1}$$

$$\rho \frac{d\boldsymbol{u}}{dt} = \operatorname{div}\mathbf{T} - \boldsymbol{\nabla} p + \rho \boldsymbol{b} \tag{2}$$

where $\boldsymbol{u}$ is the velocity field, p is the pressure, ρ is the (constant) density and $\mathbf{T}$ is the Cauchy stress tensor.

2.2 Constitutive equations

To be able to solve this system a constitutive law for the stress tensor $\mathbf{T}$ should be specified. Different choices could be made at this stage to take into account the specific fluid behavior. The commonly used constitutive models are the following:

1. ***Navier-Stokes*** *(Newtonian fluids)*

$$\mathbf{T} = 2\mu\mathbf{D} \tag{3}$$

Here $\mathbf{D}$ represents the symmetric part of velocity gradient and μ denotes the dynamical viscosity. Introducing (3) into the momentum balance (2) leads to the well known classical Navier-Stokes system.

2. ***Maxwell fluids***

$$\mathbf{T} + \lambda\frac{\delta\mathbf{T}}{\delta t} = 2\mu\mathbf{D} \tag{4}$$

This model is considered as the first approach to the viscoelastic fluid behavior. The ratio between viscous and elastic coefficients is hidden in the parameter λ. This parameter has the dimension of time and is usually referred as *relaxation time*. The symbol $\frac{\delta\cdot}{\delta t}$ stands for the so–called *convected derivative*, which is an objective time-derivative (see section 2.3 for details).

3. ***Oldroyd type fluids***
Combining the previous two models the behavior of incompressible viscous and viscoelastic fluids can be described. In this case the constitutive equation will take the form:

$$\mathbf{T} + \lambda_1\frac{\delta\mathbf{T}}{\delta t} = 2\mu\left(\mathbf{D} + \lambda_2\frac{\delta\mathbf{D}}{\delta t}\right) \tag{5}$$

It is possible to show that this model contains the former two models as special cases, for certain choices of λ_1 and λ_2.

2.3 Convected derivative

To guarantee that the model is objective, i.e. invariant to Galilean transform, the convected derivative should be used instead of the material time-derivative, but this is not the only possibility. The general expression for the convected derivative of a tensor $\mathbf{M}$ is the following:

$$\begin{aligned}\left(\frac{\delta\mathbf{M}}{\delta t}\right)_{abc} &= \dot{\mathbf{M}} - \mathbf{WM} + \mathbf{MW} + a(\mathbf{DM} + \mathbf{MD}) \\ &+ b(\mathbf{D} : \mathbf{M})\mathbf{I} + c(\mathbf{D}\ \mathrm{tr}\mathbf{M})\end{aligned} \tag{6}$$

In this expression a, b and c are real parameters, and thus we have three-parametric family of convected derivatives. Such a general form of convected derivative leeds to so called Oldroyd 8-constant model (see. [11], [12] or [3]). Usually the choice of a convected derivative is reduced to cases where $b = 0$ and $c = 0$. This corresponds to some frequently used derivatives listed in the Table 1 below:

Name	Definition	a
Lower-convected	$\overset{\triangle}{\mathbf{M}} = \dot{\mathbf{M}} + \mathbf{L}^T\mathbf{M} + \mathbf{ML}$	1
Upper-convected	$\overset{\triangledown}{\mathbf{M}} = \dot{\mathbf{M}} - \mathbf{LM} - \mathbf{ML}^T$	-1
Co-rotational	$\overset{\circ}{\mathbf{M}} = \dot{\mathbf{M}} - \mathbf{WM} + \mathbf{MW}$	0

Table 1: Commonly use convected derivatives

The one-parametric family of convected derivatives can be then written as:

$$\left(\frac{\delta\mathbf{M}}{\delta t}\right)_a = \dot{\mathbf{M}} - \mathbf{WM} + \mathbf{MW} + a(\mathbf{DM} + \mathbf{MD}) \tag{7}$$

This is sometimes referred as the Gordon-Schowalter derivative with parameter $a = \xi - 1$, $a \in \langle -1; 1\rangle$ where ξ is called *slip parameter*.

2.4 Shear-thinning viscosity

One of the generally accepted properties of blood flow is its shear-thinning behavior, which is mainly due to aggregation and deformability of erythrocytes (RBCs). In particular, at rest or at low shear rates, blood seems to have a high apparent viscosity (due to RBCs aggregation into clusters called rouleaux) while at high shear rates the cells become disaggregated and deform into an infinite variety of shapes without changing volume (deformability of RBCs), resulting in a reduction in the blood Rs viscosity. Moreover blood cells are essentially elastic membranes filled with a fluid and it seems reasonable, at least under certain flow conditions, to expect blood to behave like a viscoelastic fluid.

If blood flow is modeled by a viscoelastic constitutive law that does not predict the shear-thinning behavior, then a specific viscosity formula respecting the shear-thinning property of blood needs to be included. Several formulas have been used in blood flow simulations and calibrated with parameters obtained by curve fitting with experimental data. A general viscosity function can be written as follows:

$$\mu(\dot{\gamma}) = \mu_\infty + (\mu_0 - \mu_\infty)F(\dot{\gamma}). \tag{8}$$

Here μ_0 and μ_∞ are the asymptotic viscosity values for low and high shear rates, respectively. The appropriate transition between these values is carried out by

the shear-rate dependent function $F(\dot{\gamma})$. This function should satisfy the following natural limit conditions:

$$\lim_{\dot{\gamma}\to 0^+} F(\dot{\gamma}) = 1 \qquad \lim_{\dot{\gamma}\to\infty} F(\dot{\gamma}) = 0$$

There are many possible choices for such a function $F(\dot{\gamma})$. One of the most frequently used is the generalized *Cross* formula included in the following model

$$\mu(\dot{\gamma}) = \mu_\infty + \frac{\mu_0 - \mu_\infty}{(1+(\lambda\dot{\gamma})^b)^a} \tag{9}$$

with parameters obtained by calibration against suitable experimental data. The following parameters have been used for blood flow simulations with this model in [9]:

$$\mu_0 = 1.6\cdot 10^{-1} Pa\cdot s \qquad \mu_\infty = 3.6\cdot 10^{-3} Pa\cdot s$$
$$a = 1.23,\ b = 0.64s \qquad \lambda = 8.2s$$

A Cross model can be used to generalize Newtonian, Maxwell or Oldroyd type constitutive laws, replacing the original constant viscosity μ by the shear-dependent viscosity $\mu(\dot{\gamma})$. In the present work we consider the generalized Navier-Stokes equations with a shear-thinning Cross viscosity of this type to model blood flow.

2.5 Clot model

The external blood coagulation pathway is triggered by contact of blood with the subendothelium layer containing the tissue factor. This starts the cascade of chemical reactions resulting in the production of fibrin. The clot is defined as a region where the fibrin concentration ($\mathsf{C_F}$) exceeds some prescribed threshold value $\mathsf{C_{CLOT}}$. This serves as an indicator of the change on the constitutive relation for blood and clot, which have different material properties. Figure 1 shows a cartoon with the modeling approach.

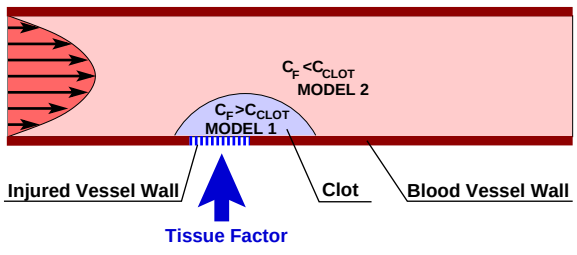

Figure 1: Clot modeling strategy

In the present simulations we have assumed that the clot viscosity is different from the blood viscosity. The biochemical model underlying clot formation was not a subject of this preliminary study and therefore the region ocupied by the clot was prescribed and fixed for all simulations.

3 Numerical Method

The numerical solution of the above described model is based on a finite-volume semi-discretization with explicit Runge-Kutta time integration. We look for a steady solution by time-marching approach, i.e. the unsteady governing system is solved with steady boundary conditions and the stationary solution is recovered when $t \longrightarrow \infty$.

The artificial compressibility formulation was used to resolve pressure and enforce the divergence-free constraint. The equation (1) is modified by adding the time-derivative of pressure properly scaled by the artificial speed of sound $\mathfrak{c}$:

$$\frac{1}{\mathfrak{c}^2}\frac{\partial p}{\partial t} + \operatorname{div} \boldsymbol{u} = 0 \tag{10}$$

3.1 Space discretization

The computational mesh is structured, consisting of hexahedral control volumes. To evaluate the viscous fluxes also dual finite volumes are needed. These have octahedral shape and are centered around the corresponding primary cell faces. See the following figure 2 for the schematic view of such configuration.

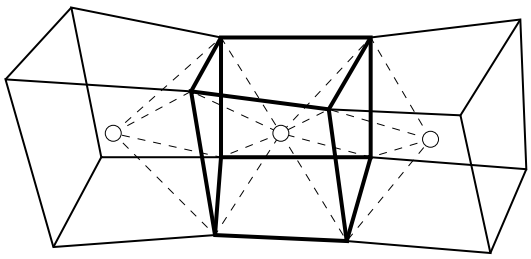

Figure 2: Finite-volume grid in 3D

The system of generalized NS equations can be rewritten in the vector form. Here we use W to denote the vector of unknowns (including pressure). Vectors F, G and H denote the inviscid fluxes in x,y,z directions, while R, S and T stand for their viscous counterparts. Using this notation, the spatial finite-volume semi-discretization in the cell D can be written in the following form:

$$\frac{\partial \mathsf{W}}{\partial t} = \frac{-1}{|D|}\oint_{\partial D}\Big[(\mathsf{F}-\mathsf{R}),(\mathsf{G}-\mathsf{S}),(\mathsf{H}-\mathsf{T})\Big]\cdot\hat{\boldsymbol{\nu}}\, dS \tag{11}$$

Here D denotes the computational cell, $\hat{\boldsymbol{\nu}}$ is the outer unit normal vector of the cell boundary, dS is the surface element of this boundary. Equation (11) can be rewritten in operator form:

$$\frac{\partial \mathsf{W}_{ijk}}{\partial t} = -\mathcal{L}\,\mathsf{W}_{i,j,k} \tag{12}$$

Here $\mathcal{L}$ stands for the finite-volume discretization operator. This operator is still exact at this stage and it must be properly discretized to allow for numerical solution. This is done by replacing the fluxes in the formulation by their numerical approximations.

The inviscid flux integral can be approximated using centered cell fluxes, e.g. the value of the flux F on the cell face with index $\ell = 1$ is computed as the average of cell-centered values from both sides of this face:

$$\mathsf{F}_1^n = \frac{1}{2}[\mathsf{F}(\mathsf{W}_{i,j,k}^n) + \mathsf{F}(\mathsf{W}_{i+1,j,k}^n)] \qquad (13)$$

The contribution of inviscid fluxes is finally summed up over the cell faces $\ell = 1, \ldots, 6$. In this way we can write the inviscid flux approximation:

$$\oint_{\partial D} \mathsf{F}\nu^x \, dy\, dz \approx \sum_{\ell=1}^{6} \mathsf{F}_\ell \nu_\ell^x S_\ell \qquad (14)$$

The discretization of viscous fluxes is a little bit more complicated since the vectors $\mathsf{R}, \mathsf{S}, \mathsf{T}$ were defined using the derivatives of velocity components and these derivatives need to be approximated at cell faces. This can be done using the dual finite-volumes centered around the corresponding faces (see Figure 2).

The evaluation of the velocity gradient components is then replaced by the evaluation of the surface integral over the dual volume boundary. Finally, this surface integral is approximated by a discrete sum over the dual cell faces (with indices $m = 1, \ldots, 8$). For example trying to evaluate the first component of the viscous flux R_1 (i.e. approximate u_x) at the cell face $l = 1$ we must proceed in the following way:

$$u_x \approx \oint_{\partial \tilde{D}} u\, \nu^x \, dy\, dz \approx \sum_{m=1}^{8} u_m \nu_m^x S_m \qquad (15)$$

The outer normal of the dual cell faces should be properly approximated $\nu^x \approx \nu_m^x$. The values of velocity components in the middle nodes of these faces are taken as an average of the values in the corresponding vertices.

3.2 Time integration

The problem is now in the semi-discrete form:

$$\frac{d\mathsf{W}_{ijk}}{dt} = -\tilde{\mathcal{L}}\, \mathsf{W}_{i,j,k}. \qquad (16)$$

This system of ordinary differential equations can be solved e.g. by the Runge-Kutta multistage method:

$$\begin{aligned} \mathsf{W}_{i,j,k}^{(0)} &= \mathsf{W}_{i,j,k}^{n} \\ \mathsf{W}_{i,j,k}^{(r+1)} &= \mathsf{W}_{i,j,k}^{(0)} - \alpha_{(r)} \Delta t \tilde{\mathcal{L}} \mathsf{W}_{i,j,k}^{(r)} \\ \mathsf{W}_{i,j,k}^{n+1} &= \mathsf{W}_{i,j,k}^{(m)} \end{aligned} \qquad (17)$$

Here $r = 1, \ldots, m$, for the m-stage method. The three-stage explicit RK scheme has coefficients: $\alpha_{(1)} = 1/2,\ \alpha_{(2)} = 1/2,\ \alpha_{(3)} = 1$.

4 Numerical Results

The computational domain represents a straight vessel of finite length. The cylinder has a diameter D=6.2 mm and length L=5D=31 mm. The region occupied by the clot is assumed to have spherical shape with center placed at 1/3 of L and has a radius equal D/2. Mean inlet velocity is $U_0 = 6.15\ cm/s$.

The numerical results presented in this paper corespond to a generalized Newtonian fluid with viscosity described in section 2.4. The results provide a qualitative study of the model behavior with respect to the ratio of clot viscosity versus blood viscosity. The clot viscosity is usually referred to be much higher than the one of blood. Thus a parameter range has been chosen for with $\mu_{Clot}/\mu_{Blood} = 1, 5, 10, 20, 40$, which seems to be sufficient for the clot formation modeling. It is obvious that for $\mu_{Clot}/\mu_{Blood} = 1$ there is no clot and the flow should tend to fully developed axisymmetric profile. The inlet velocity profile is prescribed as an exact solution of Newtonian flow at viscosity μ_∞. This leeds to some minor non-Newtonian velocity profile adjustment close to inlet as it can bee seen in Figure 3.

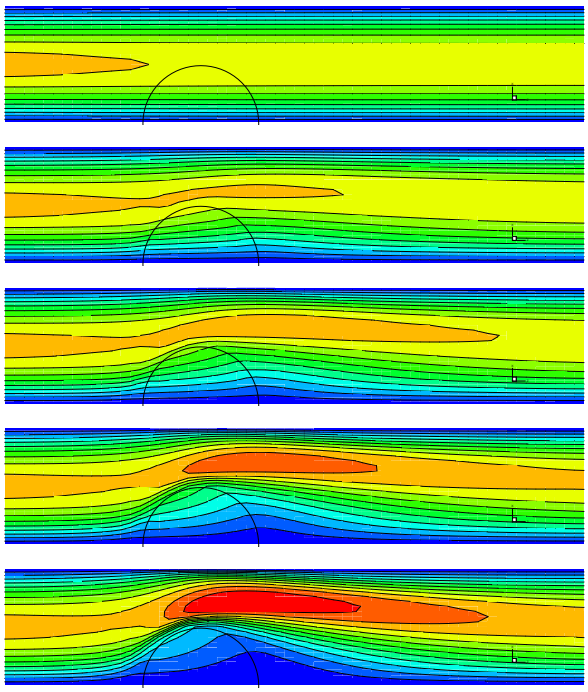

Figure 3: Axial velocity contours in the vessel symmetry plane for viscosity ratio $\mu_{Clot}/\mu_{Blood} = 1, 5, 10, 20, 40$ (from top to bottom).

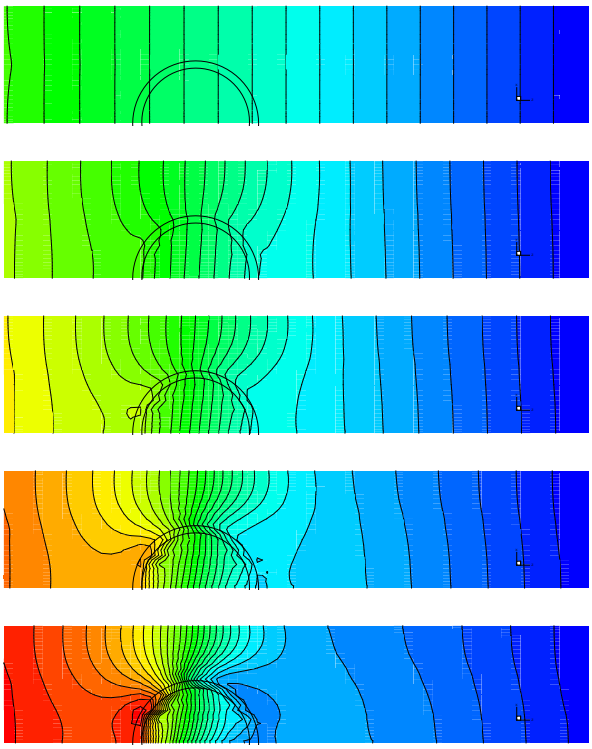

Figure 4: Pressure contours in the vessel symmetry plane for viscosity ratio $, 5, 10, 20, 40$ (from top to bottom).

It is important to note that the shear-thinning behavior of blood reinforces the simulated clot effect. The local increase of viscosity causes flow deceleration and results in decrease of the local shear rate. Lower shear-rate leeds to further viscosity increase due to shear-thinning.

The semi-spherical shape of the simulated clot leeds to important three-dimensional flow structure in the proximity of the artificial obstacle. This can be detected from velocity contours shown in transversal sections. The placement of these sections is shown in Figure 5.

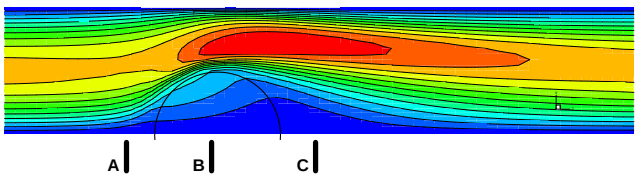

Figure 5: Section placement with respect to clot area.

The axial velocity contours in the case $\mu_{Clot}/\mu_{Blood} = 40$ are shown in Figure 6.

The incoming velocity profile symmetry is broken by the asymmetrically placed clot region. This can be seen in the shift of the maximal velocity from the center of the cross-section.

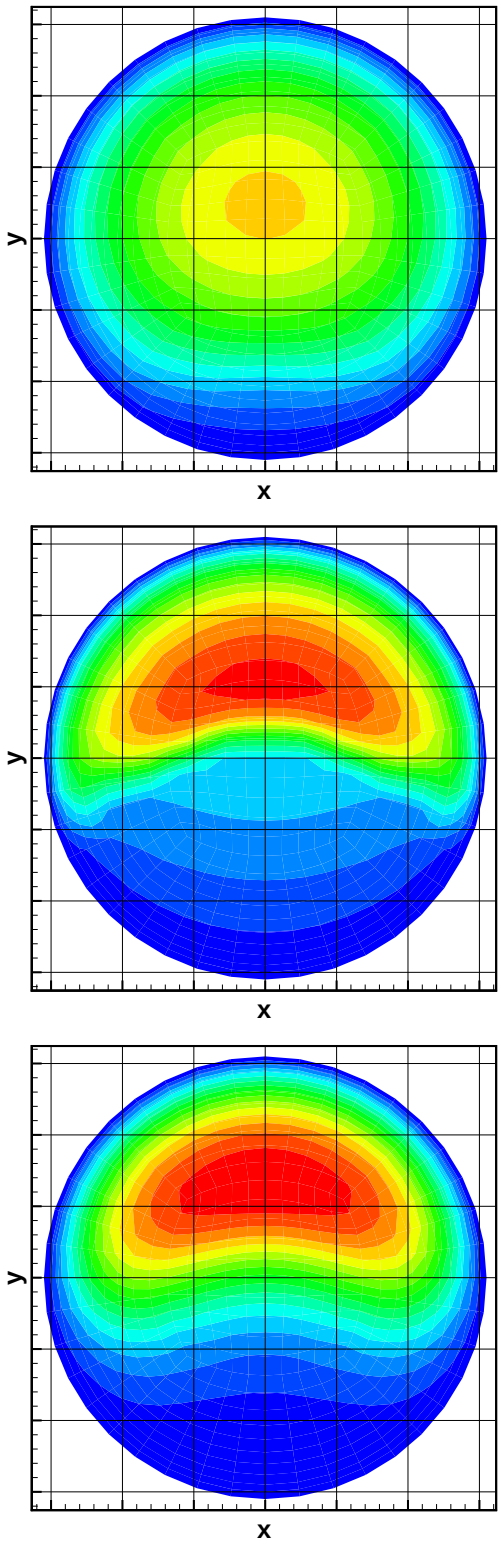

Figure 6: Axial velocity contours in the sections A, B and C for $\mu_{Clot}/\mu_{Blood} = 40$

5 Conclusion and Comments

- Numerical results have shown the expected behavior of flow field in the vicinity of simulated clot. Simple change in local viscosity leeds to required behavior typical for solid obstacles of impermeable or porous media type.
- More details on the numerical method used and corresponding numerical results will be provided in a forthcoming paper.
- The fixed (prescribed) clot shape will be further replaced by an appropriate fibrin concentration isosurface resulting from the solution of coupled biochemistry model. The time dependent increase in fibrin concentration can be reflected by the appropriate increase in local viscosity ratio.
- Future extension of this work will follow the unsteady (pulsatile) blood flow behavior in living organisms. The unsteady extension of presented solvers is crucial for future realistic calculations of flow and flow-structure problems.
- The same approach to the shear-thinning blood behavior could be adopted also for more complex rheological constitutive laws (e.g. for viscoelastic models). The non-linearity of such complex model could leed to formation of unexpected clot shapes due to viscoelastic extra stress.

Acknowledgments: The financial support for the present work was partly provided by the European research project **HaeMO$\partial\varepsilon$l** HPRN-CT-2002-002670 and by the Research Plan *MSM 6840770010* of the *Ministry of Education of Czech Republic*.

References:

[1] M. Anand, K. Rajagopal, and K. R. Rajagopal. A model incorporating some of the mechanical and biochemical factors underlying clot formation and dissolution in flowing blood. *Journal of Theoretical Medicine*, 5(3–4):183–218, September–December 2003.

[2] M. Anand and K. R. Rajagopal. A mathematical model to describe the change in the constitutive character of blood due to platelet activation. *Comptes Rendues Mechaniques*, 330:557–562, 2002.

[3] R. B. Bird, R. C. Armstrong, and O. Hassager. *Dynamics of polymeric liquids*, volume 1. John Willey & Sons, second edition, 1987.

[4] S. Butenas and K. G. Mann. Blood coagulation. *Biochemistry (Moscow)*, 67(1):3–12, 2002. Translated from Biokhimiya, Vol. 67, No. 1, 2002, pp. 5–15.

[5] A. L. Fogelson and A. L. Kuharsky. Membrane binding site density can modulate activation thresholds in enzyme systems. *Journal of Theoretical Biology*, 193:1–18, 1998.

[6] P. A. Gentry. Comparative aspects of blood coagulation. *The Veterinary Journal*, 168:238–251, 2004.

[7] A. L. Kuharsky. *Mathematical Modelling of Blood Coagulation*. PhD thesis, University of Utah, 1998.

[8] A. L. Kuharsky and A. L. Fogelson. Surface-mediated control of blood coagulation: The role of binding site densities and platelet deposition. *Biophysical Journal*, 80:1050–1074, March 2001.

[9] A. Leuprecht and K. Perktold. Computer simulation of non-Newtonian effects of blood flow in large arteries. *Computer Methods in Biomechanics and Biomechanical Engineering*, 4:149–163, 2001.

[10] L. A. Norris. Blood coagulation. *Best Practice & Research Clinical Obstetrics & Gynaecology*, pages 369–383, 2003.

[11] J. G. Oldroyd. On the formulation of rheological equations of state. *Proceedings of Royal Society, London, Ser. A*, 200:523–541, 1950.

[12] J. G. Oldroyd. Non-Newtonian effects in steady motion of some idealized elastico-viscous liquids. *Proceedings of Royal Society, London, Ser. A*, 245:278–297, 1958.

[13] N.-T. Wang and A. L. Fogelson. Computational methods for continuum models of platelet aggregation. *Journal of Computational Physics*, 151:649–675, 1999.

[14] V. I. Zarnitsina, A. V. Pokhilko, and F. I. Ataullakhanov. A mathematical model for the spatio-temporal dynamics of intrinsic pathway of blood coagulation - i. the model description. *Thrombosis research*, 84(4):225–236, 1996.

[15] V. I. Zarnitsina, A. V. Pokhilko, and F. I. Ataullakhanov. A mathematical model for the spatio-temporal dynamics of intrinsic pathway of blood coagulation - ii. results. *Thrombosis research*, 84(5):333–344, 1996.